J|A|C|S
ARTICLES

Published on Web 08/26/2008

Fermi Level Engineering of Single-Walled Carbon Nanotubes by $AuCl_3$ Doping

Ki Kang Kim,[†] Jung Jun Bae,[†] Hyeon Ki Park,[†] Soo Min Kim,[†] Hong-Zhang Geng,[†] Kyung Ah Park,[†] Hyeon-Jin Shin,[†,‡] Seon-Mi Yoon,[‡] Anass Benayad,[§] Jae-Young Choi,*[,‡] and Young Hee Lee*[,†]

BK21 Physics Division, Center for Nanotubes and Nanostructured Composites, Sungkyunkwan Advanced Institute of Nanotechnology, Sungkyunkwan University, Suwon 440-746, Republic of Korea, Display Device and Processing Laboratory, Samsung Advanced Institute of Technology, P.O. Box 111 Suwon, 440-600, Republic of Korea, and Analytic Engineering Center, Samsung Advanced Institute of Technology, P.O. Box 111 Suwon, 440-600, Republic of Korea

Received May 23, 2008; E-mail: jaeyoung88.choi@samsung.com (J.Y.C.); leeyoung@skku.edu (Y.H.L.)

Abstract: We investigated the modulation of optical properties of single-walled carbon nanotubes (SWCNTs) by $AuCl_3$ doping. The van Hove singularity transitions (E_{11}^S, E_{22}^S, E_{11}^M) in absorption spectroscopy disappeared gradually with an increasing doping concentration and a new peak appeared at a high doping concentration. The work function was downshifted up to 0.42 eV by a strong charge transfer from the SWCNTs to $AuCl_3$ by a high level of p-doping. We propose that this large work function shift forces the Fermi level of the SWCNTs to be located deep in the valence band, i.e., highly degenerate, creating empty van Hove singularity states, and hence the work function shift invokes a new asymmetric transition in the absorption spectroscopy from a deeper level to newly generated empty states.

1. Introduction

Single-walled carbon nanotubes (SWCNTs) have semiconducting and metallic properties depending on the chirality of the nanotubes.[1,2] Of particular interest is the semiconducting nature of nanotubes that can be utilized for nanoscale semiconductor devices. Excellent device performance has been demonstrated on an isolated SWCNT that act as a field-effect transistor with a high on/off ratio of 10^6 and mobility of up to 220 cm^2/V s.[3] A semiconducting SWCNT device usually reveals a p-type in ambient conditions that can be attributed to gas adsorbates and an n-type in a vacuum.[4]

Doping of CNTs is very different from that of conventional semiconducting materials where the foreign impurity material is incorporated into the host material and the doping level is determined by the solubility of the impurity within the host material. In contrast, all of the host carbon atoms in SWCNTs are exposed to the nanotube surface, making it difficult for them to incorporate foreign atoms to substitutional or interstitial sites due to large activation energy. For this reason, doping of CNTs by the substitution of carbon atoms with foreign atoms such as nitrogen or boron has been rare let alone controlling the doping level.[5] Instead, adsorbates such as atoms, molecules, and polymers with appropriate functional groups have been introduced on the nanotube surface.[5–9] The main effect is the to-and-fro motion of electrons between adsorbates and CNTs that eventually causes a Fermi level shift.[10] The amount of electron transfer determines the doping level or the Fermi level shift of the CNTs. Unlike a conventional metal oxide semiconductor field effect transistor (MOSFET) that involves a charge depletion layer, a CNT device is operated as a Schottky barrier FET where the current is exclusively determined by Schottky barrier engineering at the junction.[11] The direction of the transferred electrons decides the doping type. The p-type CNTs are presumably caused by the electron-accepting adsorbates that downshift the Fermi level toward valence bands of nanotubes.

The purpose of this study, described in this paper, is threefold: (i) to control the doping level precisely, (ii) to extract information about the doping level, and (iii) to apply the concepts we learn to conducting film to improve the film's conductivity. We

[†] Sungkyunkwan University.
[‡] Display Device and Processing Laboratory in SAIT.
[§] Analytic Engineering Center in SAIT.

(1) An, K. H.; Lee, Y. H. *NANO* **2006**, *1*, 115–138.
(2) Saito, R.; Fujita, M.; Dresselhaus, G.; Dresselhaus, M. S. *Appl. Phys. Lett.* **1992**, *60*, 2204–2206.
(3) Martel, R.; Schmidt, T.; Shea, H. R.; Hertel, T.; Avouris, Ph. *Appl. Phys. Lett.* **1998**, *73*, 2447–2449.
(4) Collins, P. G.; Bradley, K.; Ishigami, M.; Zettl, A. *Science* **2000**, *287*, 1801–1804.
(5) Javey, A.; Wang, Q.; Ural, A.; Li, Y.; Dai, H. *Nano Lett.* **2002**, *2*, 929–932.
(6) Chen, Z.; Appenzeller, J.; Lin, Y. M.; Sippel-Oakley, J.; Rinzler, G.; Tang, J.; Wind, S. J.; Solomon, P. M.; Avouris, Ph. *Science* **2006**, *311*, 1735.
(7) Kong, J.; Soh, H. T.; Cassell, A. M.; Calvin, C. F.; Dai, H. *Nature* **1998**, *395*, 878–881.
(8) Carroll, D. L.; Redlich, Ph.; Blase, X.; Chalier, J.-C.; Curran, S.; Ajayan, P. M.; Roth, S.; Ruhle, M. *Phys. Rev. Lett* **1998**, *81*, 2332–2335.
(9) Derycke, V.; Martel, R.; Appenzeller, A.; Avouris, Ph. *Appl. Phys. Lett.* **2002**, *80*, 2772–2775.
(10) Martel, R.; Derycke, V.; Lavoie, C.; Appenzeller, J.; Chan, K. K.; Tersoff, J.; Avouris, Ph. *Phys. Rev. Lett.* **2001**, *87*, 256805/1-4.
(11) Klinke, C.; Chen, J.; Afzali, A.; Avouris, Ph. *Nano Lett.* **2005**, *5*, 555–558.

chose $AuCl_3$ to modulate the doping level of the SWCNTs. The effect of doping on the electronic structures of SWCNTs was investigated by UV−vis−NIR absorption, Raman, and ultraviolet photoelectron spectroscopy. We interpreted the disappearance and a new appearance of some peaks in terms of a Fermi level shift deep into the valance band at a high doping concentration. This also explains well why the surface resistance of the film was reduced by about 90% after such heavy doping.

2. Sample Preparation and Experimental Methods

Highly purified arc discharge SWCNTs with a mean diameter of 1.4 nm and purity of 93 wt %, purchased from Iljin Nanotech Co., Ltd., were used in this experiment. To prepare homogeneous thin CNT films, SWCNTs of 1 mg were added in 30 mL of 1,2-dichloroethane followed by sonication in a bath type sonicator (RK 106, Bandelin Electronic, Berlin, Germany) for 6 h.[12] This solution was centrifuged (Hanil Science Industrial Co., Ltd., Mega 17R) at 8000 rpm for 10 min. The supernatant of the resulting solution was sprayed on a quartz substrate (2×2 cm^2) with an argon gas brush pistol (Gunpiece GP-1). The prepared SWCNT film was annealed at 900 °C for 1 h in an Ar atmosphere to exclude the solvent effect.[13] This sample was assigned to the pristine sample.

We chose $AuCl_3$ to control the doping level of the SWCNTs. The reduction potential has the following relationship to the work function (φ), $\varphi/e = V$ (vs NHE) + 4.44, where φ is the work function and V is the reduction potential vs a Normal Hydrogen Electrode (NHE).[14,15] Since the reduction potential of the Au^{3+} ion is 1.52 V, higher than those of SWCNTs with diameter ranges of 1.3−1.5 nm, the charge transfer from SWCNTs to Au^{3+} ions is expected to naturally occur.[14–16] We prepared the doping solvents with various concentrations of $AuCl_3$ (Sigma-Aldrich) in nitromethane. Each doping solvent of 400 μL was dropped onto the prepared SWCNTs film. After 30 s of residual time, the solvent was spin-coated at 2500 rpm for 60 s (Midas System, Spin 2,000).

UV−vis−NIR absorption spectroscopy (Varian, Cary 5000) and Raman spectroscopy (Renisaw, RM-100 Invia) with excitation energies of 1.96 and 2.41 eV were used for characterizing the optical properties of the doped SWCNTs. The work functions were measured by ultraviolet photoelectron spectroscopy (UPS) using a He I discharge lamp ($h\nu$ = 21.2 eV) (Gammadata VUV 5050). The work functions were measured from the secondary-electron cutoff of the UPS using gold metal as a reference. The Fermi level position was calibrated by measuring the Fermi edge of gold metal. The sheet resistance was measured by a four-point method (Keithley 2000 meltimeter) at room temperature.

3. Results and Discussion

Figure 1 shows the UV−vis−NIR absorption spectra doped with various concentrations of $AuCl_3$. Three van Hove singularity-related transition peaks, E_{11}^S, E_{22}^S, and E_{11}^M, were clearly observed in the pristine sample. As mentioned before, the Au^{3+} ions have larger reduction potentials (or work functions) than SWCNTs with diameters of 1.3−1.5 nm, and therefore most nanotubes within this diameter range are likely to be oxidized at a high doping concentration independent of metallicity.[17] At a low doping concentration, the van Hove singularity near the Fermi level was modified first, i.e., the E_{11}^S peak intensity was reduced first. At 10 mM, the E_{11}^S peak intensity disappeared completely and the second peak E_{22}^S began to be shifted to a higher energy side that eventually disappeared at 30 mM. Even the E_{11}^M peak disappeared at 60 mM. More interestingly, a new peak appeared near 1.12 eV. This state remained unchanged even at a higher doping concentration.

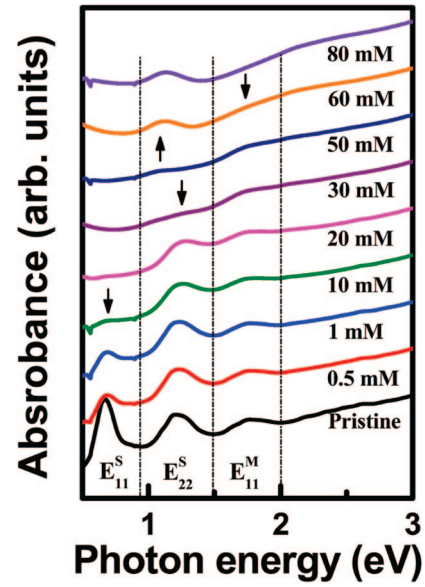

Figure 1. (a) UV−vis−NIR optical absorption spectra with increasing $AuCl_3$ concentration. The arrows indicate the disappearance of van Hove singularity transitions of p-doped SWCNTs and the appearance of the new peak induced at highly p-type doping. $E_{ii}^{S(M)}$ indicates the Van Hove singularity transitions between the i^{th} energy levels of the semiconducting (metallic) SWCNT.

The effect of doping was clearly shown in resonant Raman spectra (Figure 2). The spectrum near 100−400 cm^{-1} is known as the radial breathing mode (RBM) originating from the breathing of the tube along the radial direction (A_{1g} phonon). This provides useful information for the diameter and chirality of tubes.[18] At an excitation energy of 2.41 eV, all of the semiconducting nanotubes were excited in the pristine sample as shown in Figure 2a. The G-band appeared near 1590 cm^{-1}. The peak positions of the G-band were not shifted appreciably at a low doping concentration up to 1 mM and were upshifted markedly by about 10 cm^{-1} at a high concentration. This change is consistent with the previous report of the phonon stiffening effect by p-type doping.[19] It is known that the intensity of the G′-band is proportional to the metallicity of the sample.[20] The effect of enhanced p-type doping was also manifested in

(12) Kim, K. K.; Bae, D. J.; Yang, C.-M.; An, K. H.; Lee, J. Y.; Lee, Y. H. *J. Nanosci. Nanotechnol.* **2005**, *5*, 1055–1059.
(13) Shin, H.-J.; Kim, S. M.; Yoon, S.-M.; Benayad, A.; Kim, K. K.; Kim, S. J.; Park, H. K.; Choi, J.-Y.; Lee, Y. H. *J. Am. Chem. Soc.* **2008**, *130*, 2062–2066.
(14) Zhao, J.; Han, J.; Lu, J. P. *Phys. Rev. B* **2002**, *65*, 193401/1–4.
(15) Okazaki, K.-I.; Nakato, Y.; Murakoshi, K. *Phys. Rev. B* **2003**, *68*, 035434/1−5.
(16) Choi, H. C.; Shim, M.; Bangsaruntip, S.; Dai, H. *J. Am. Chem. Soc.* **2002**, *124*, 9058–9059.
(17) O'Connell, M. J.; Eibergen, E. E.; Doorn, S. K. *Nat. Mater.* **2005**, *4*, 412–418.
(18) Dresselhaus, M. S.; Dresselhaus, G.; Saito, R.; Jorio, A. *Phys. Rep.* **2005**, *409*, 47–99.
(19) Rao, A. M.; Eklund, P. C.; Bandow, S.; Thess, A.; Smalley, R. E. *Nature* **1997**, *388*, 257–259.
(20) Kim, K. K.; Park, J. S.; Kim, S. J.; Geng, H.-Z.; An, K. H.; Yang, C.-M.; Sato, K.; Saito, R.; Lee, Y. H. *Phys. Rev. B* **2007**, *76*, 205426/1–8.

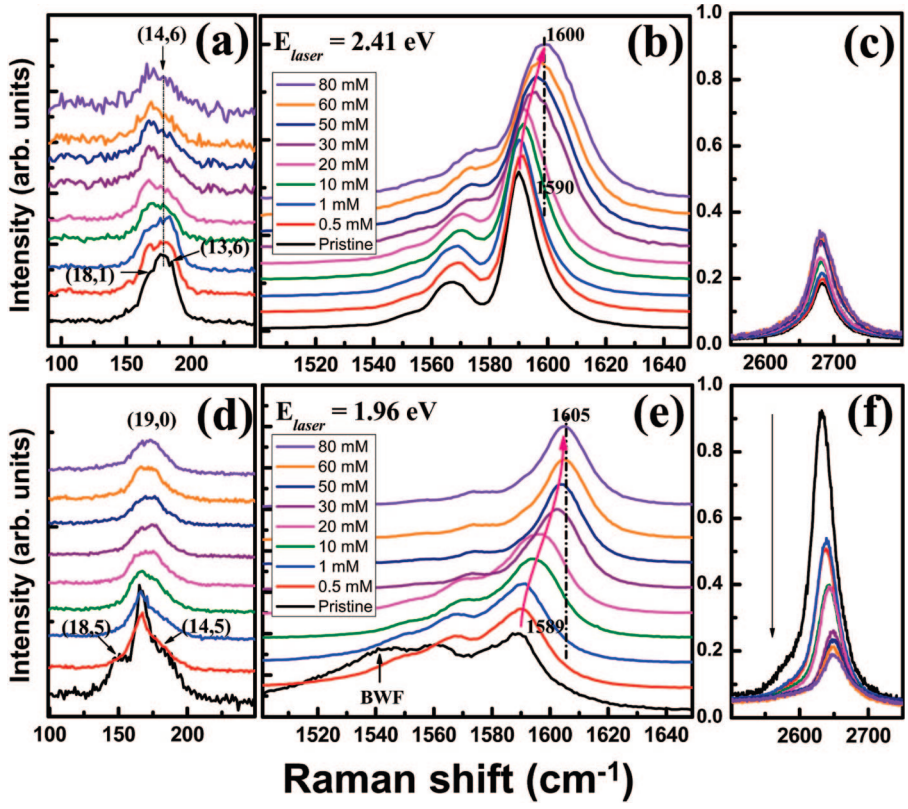

Figure 2. Raman spectra of $AuCl_3$-doped SWCNTs at an excitation energy of (a−c) 2.41 eV and (d−f) 1.96 eV, respectively. (a) and (d) are the respective radial breathing modes (RBMs). The (*n*,*m*) in parentheses indicates the chiral indices of the SWCNTs. (b) and (e) are the respective G-bands. (c) and (f) are the respective G′-bands. All Raman spectra were normalized by the G-band intensity. The arrow shows the decrease of G′-band intensity with increasing $AuCl_3$ concentration.

the slightly increased intensity of the G′-band near 2670 cm^{-1}, implying highly degenerate p-type doping. A similar phenomenon was observed with different laser excitation (1.96 eV) illustrated in Figure 2d−f. In this case, some portion of the metallic SWCNTs indicated by (14, 5) in this figure were excited in the pristine sample. Accordingly, the characteristic metallic peak with a long tail at the lower energy side of the G-band, known as a Breit−Wigner−Fano (BWF) line shape originating from coupling of the discrete phonons to an electronic continuum, was visible as seen in Figure 2e.[21] It is interesting to note that the BWF line shape was diminished immediately at a low doping concentration of 0.5 mM and disappeared completely at a high doping concentration. The G-band shift was also similar to those at an excitation energy with 2.41 eV but to a large shift up to 15 cm^{-1} in this case. The abrupt shift of the G-band at 30 mM is strongly correlated to the disappearance of E_{22}^S in Figure 1. The reduction of metallicity was also observed in the decreased intensity of the G′-band. The lessons learned from these observations are (i) doping in metallic SWCNTs occurs immediately at a low doping concentration; (ii) the upshift of the G-band peak indicates p-type doping; and (iii) the stepwise upshift of the G-band peak is strongly correlated to the disappearance of the characteristic absorption peak.

Figure 3 shows the work function changes obtained from the UPS and the sheet resistance at various $AuCl_3$ concentrations. The work function increased by 0.42 eV to saturate to 4.73 eV at a high doping concentration from 4.31 eV of the pristine sample. This trend of an increasing work function with doping is again consistent with the previous report for the p-type doping.[22] On the other hand, the sheet resistance of the conducting film decreased rapidly about 60% at a low doping concentration and saturated further, reaching about 90% of the resistance reduction (see Supporting Information Table S1). The trends of the changes of the two quantities were exactly opposite to each other. The underlying mechanism for the reduction of sheet resistance can be explained in terms of the random network of SWCNTs in the film. The work function of the metallic tubes is presumably smaller than that of the semiconducting tubes.[14,23] It is worth reporting that the electrochemical Raman measurements gave a larger work function in metallic tubes than in semiconducting ones.[15] Since the sample was dispersed using SDS in aqueous medium and furthermore only few nanotubes were measured, the former results were chosen in our analysis. The pristine semiconducting nanotube is p-type under ambient conditions. The possible Schottky barrier between metallic and semiconducting nanotubes is formed, as illustrated in the schematic of Figure 3b. In general, the sheet resistance of the CNT network film consists of the sum of the resistances of the nanotubes, itself, and the contact resistances between the nanotubes. The contact resistance is governed by a Schottky barrier formed between the metallic and semiconducting nanotubes as shown in Figure 3c. At a low doping concentration, the Fermi levels of both metallic and semiconducting nanotubes

(21) Brown, S. D. M.; Jorio, A.; Corio, P.; Dresselhaus, M. S.; Dresselhus, G.; Saito, R.; Kneipp, K. *Phys. Rev. B* **2001**, *63*, 155414/1–8.

(22) Kong, B.-S.; Jung, D.-H.; Oh, S.-K.; Han, C.-S.; Jung, H.-T. *J. Phys. Chem. C* **2007**, *111*, 8377–8382.

(23) Kim, K. S.; Bae, D. J.; Kim, J. R.; Park, K. A.; Lim, S. C.; Kim, J.-J.; Choi, W. B.; Park, C. Y.; Lee, Y. H. *Adv. Mater.* **2002**, *14*, 1818–1821.

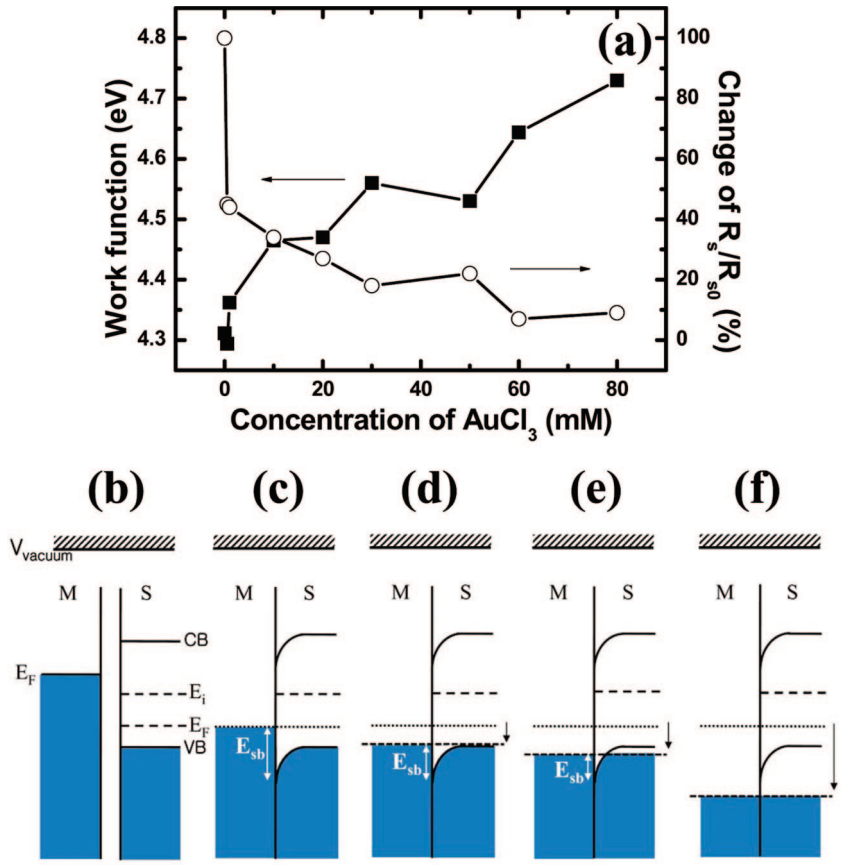

Figure 3. (a) Work function and sheet resistance at various $AuCl_3$ concentrations. A schematic diagram of the junction formation between the metallic and semiconducting SWCNTs in the SWCNT network with (b) a noncontact model, (c) the junction in the pristine sample, and (d−f) the junction with increasing $AuCl_3$ concentration. The Vacuum, E_i, E_F, C_B, V_B, and E_{sb} indicate the vacuum level, the intrinsic Fermi level, the Fermi level after p-doping, the conduction band, the valance band, and the Schottky barrier, respectively.

are shifted down toward the valence band by the same amount as the increased work function. This reduces the Schottky barrier height, resulting in the 60% of resistance reduction via $J = A^*T^2e^{-qE_{sb}/kT}(e^{qV/kT} - 1)$, where J is the current density, A^* is the effective Richardson constant (in units of $A/K^2 \cdot cm^2$), T is the absolute temperature, q is the charge, E_{sb} is the Schottky height, and V is the applied voltage.[24] The current is mostly governed by the Schottky barrier height in the exponent. When we further increased the doping concentration, the Fermi levels of SWCNTs (not only metallic but also semiconducting tubes) were further shifted down deep into the valence band. In this case, no Schottky barrier height exists, achieving 90% of the sheet resistance reduction. Therefore, the sheet resistance is no longer Schottky barrier height-dependent. This behavior is similar to that of heavily degenerate semiconductors. The sheet resistance is determined only by the carrier concentration of metallic and semiconducting tubes near the Fermi level.

The disappearance of van Hove singularity transitions and the new peak appearance with doping concentration are strongly related to the Fermi level shift. Figure 4 shows the density of states (DOSs) of (19,0) and (14,5) calculated by a local-density approximation.[25] When increasing the p-doping concentration, the van Hove singularity transitions disappeared gradually and the work function of the SWCNTs increased, as summarized in Table 1. The effect of the Fermi level shift in the electronic DOSs is illustrated in Figure 4. We presume that the position of the Fermi level of (19,0) in Figure 4(a) was −0.18 eV because the SWCNTs are p-doped under ambient conditions.[4] At 10 mM $AuCl_3$, the E_{11}^S transition was quenched in the UV−vis−NIR absorption spectra and the work function increased by 0.15 eV. This indicates that the first van Hove singularity v_1 becomes an empty state. At 30 mM $AuCl_3$, the Fermi level was further shifted down below the second van Hove singularity position marked by the red color in Figure 4a, resulting in the disappearance of E_{22}^S in the absorption spectra. The Fermi level of the metallic tubes is simultaneously shifted down, but the first van Hove singularity of the metallic tubes is located below the Fermi level. At 80 mM $AuCl_3$, the work function change of 0.42 eV moves the Fermi level further down below the first van Hove singularity of metallic tubes, resulting in the disappearance of the E_{11}^M peak in the absorption spectra. The new peak, around 1.12 eV, at a high p-doping concentration in the absorption spectra may originate from different transitions. In principle, only E_{ii} transitions are allowed by the selection rules.[26] However, in our case, the dopants are adsorbed on the nanotube wall and therefore the selection rules are no longer valid. This allows a new set of transitions. As shown in Figure 4, various types of transitions from deeper energy levels to a newly empty $v_{1'}$ could occur. For instance, one possible transition is $E_{41'}$ that gives rise to a transition energy of 1.08 eV which is close to our observed value of 1.12 eV. Further study with selection

(24) Sze, S. M. *Physics of Semiconductor Devices*, 2nd ed.; Wiley: New York, 1981; Chapter 7, pp 231−234.
(25) Akai, Y.; Saito, S. *Physica E* **2005**, *29*, 555–559.
(26) Bozovic, I.; Bozovic, N.; Damnjanovic, M. *Phys. Rev. B* **2000**, *62*, 6971–6974.

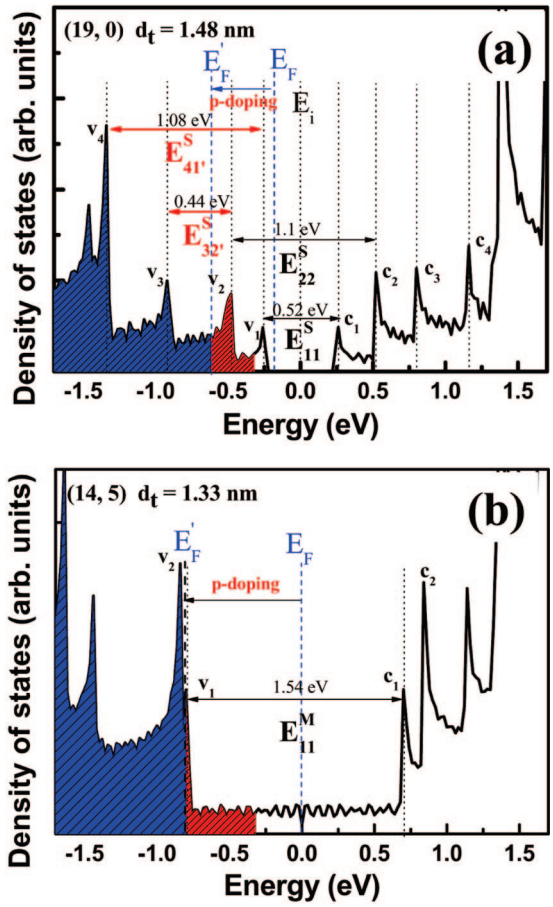

Figure 4. Density of states of (a) (19,0) and (b) (14,5) calculated by the local-density approximation. The v_i, c_i, E_i, E_F, and $E_{F'}$ indicate i^{th} levels of the valance band, conduction band, intrinsic Fermi level, Fermi level of the pristine sample, and Fermi level after p-doping, respectively.

rules upon doping is required to analyze the new transitions. At a high doping concentration of gold, the physisorbed gold ions are reduced to neutral gold particles (see Supporting Information Figure S1).

Table 1. Various Values As a Function of the $AuCl_3$ Concentration Extracted from Optical Absorption Spectra, Raman Spectra, and UPS

		G-band shifts (cm^{-1})		
$AuCl_3$(mM)	transitions	2.41 eV	1.96 eV	work function (eV)
pristine	E_{11}^S, E_{22}^S, E_{11}^M	1590	1589	4.31
10	E_{22}^S, E_{11}^M	1592	1594	4.46
30	E_{11}^M	1596	1602	4.56
60	$E_{41'}^S$	1598	1605	4.64
80	$E_{41'}^S$	1600	1605	4.73

4. Conclusions

We studied the modulation of the optical properties of SWCNTs by p-type doping using a $AuCl_3$ solution. We explained the disappearance and a new appearance of van Hove singularity related peaks in the absorption spectra that were caused by the work function changes of the nanotubes. This allowed us to perform Fermi level engineering of nanotubes. We applied the concepts learned directly to the SWCNT network film where the sheet resistance was systematically reduced with the increasing doping concentration. The Fermi level engineering of carbon nanotubes opens new vistas for many application areas involving electronic devices.

Acknowledgment. This work was financially supported by the KOSEF through CNNC at SKKU, the 21st Century Frontier R&D Program, and the STAR faculty project from the Ministry of Education.

Supporting Information Available: The D-band change of the SWCNTs in the Raman spectra after adsorbing the gold particles on the nanotube walls and the absolute sheet resistance as a function of the concentration of $AuCl_3$. This material is available free of charge via the Internet at http://pubs.acs.org.

JA8038689